APPLICATION OF ELECTRICAL RESISTIVITY METHOD IN DELINEATING GEOLOGICAL BOUNDARY IN KAKARA VILLAGE, GEZAWA LOCAL GOVERNMENT KANO, NIGERIA

BY

ABUBAKAR IBRAHIM GARBA

M.Sc./SCIEN/03895/2008-09

P13CPY8034

A THESIS SUBMITTED TO THE POSTGRADUATE SCHOOL,

IN PARTIAL FULFILMENT FOR THE AWARD OF MASTERS OF SCIENCE DEGREE IN APPLIED GEOPHYSICS.

DEPARTMENT OF PHYSICS

AHMADU BELLO UNIVERSITY, ZARIA

NIGERIA.

JUNE, 2015

DECLARATION

I declare that the work in the thesis entitled Application of Electrical Resistivity Method In Delineating Geological Boundary in Kakara Village Gezawa has been performed by me in the Department of Physics under the supervision of Dr. A.L. Ahmed and Dr K.M. Lawal The information derived from the literature has been duly acknowledged in the text and a list of references provided. No part of this thesis was previously presented for another degree or diploma at any University.

ABUBAKAR IBRAHIM GARBA

---------- ---------- ----------

Signature Date

CERTIFICATION

This thesis entitled APPLICATION OF ELECTRICAL RESISTIVITY METHOD IN DELINEATING GEOLOGICAL BOUNDARY IN KAKARA VILLAGE, GEZAWA LOCAL GOVERNMENT KANO, NIGERIA by Abubakar Ibrahim Garba meets the regulations governing the award of the degree of Masters of Science of Ahmadu Bello University, Zaria, and is approved for its contribution to knowledge and literary presentation.

_____

Dr. A.L. Ahmed Date_____
Chairman, Supervisory Committee

_____

Prof. K. M. Lawal Date_____

Member, Supervisory Committee

_____

Dr. Umar Sadiq Date_____

Head of Department

_____

Prof. A.Z. Hassan Date_____

Dean, Postgraduate School

ACKNOWLEDGEMENT

All praise is to Allah the almighty who gave me the wisdom, courage and understandings to come to the end of this research work. I am grateful to my supervisors Dr. A.L Ahmed and Prof. K.M. Lawal for their constructive criticisms and patience to thoroughly read the manuscript and make all necessary corrections. My special thank go to the management of Tahir Water under chairmanship of Alhaji Salisu Tahir (Santalin Chiroman Kano) for their unlimited support throughout this work. Special regards goes to my only mum Hajiya Hafsat and her sisters Hajiya Talatu and Hajiya Ramatu for their unrelenting support. My acknowledgement also goes to my wife Hannatu for her understanding. I also acknowledged the contribution of Baba Ali and the rest of my uncles and Mafi with all my sisters and brothers during the course of this study. I would also appreciate the support of my only course mate Aliyu. My appreciation goes to all lecturers of the department particularly Dr. C. C. Chiemeke, Dr. Sadiq, Dr. R. Nasiru, and Dr. P. O. Sule. May Almighty God reward you all. I wish to thank Zahradden, Abubakar Khalid, Sulaiman Dambam and all my friends for their untiring support may God in his infinite mercy reward too.

ABSTRACT

Geological mapping and Electrical resistivity soundings were carried out in Kakara village in Gezawa Local Government of Kano State, in order to delineate the geological boundary between the Basement Complex and the Sedimentary rock. The area is a contact zone between sedimentary rock of Chad formation and basement complex rock of Northern Nigeria. Twenty four (24) vertical electrical soundings (VES) were performed along two profiles A and B, adopting Schlumberger electrode configuration with half current separation (AB/2) varying from 1.5m to 70.0m. The geological mapping of the area shows that the area is characterized by two rock types basement complex (granite) and Chad formation (which is a sequence of sand and clay).

Interpretation was performed using computer software IX1D, the observed rocks during the geological mapping and borehole data drilled close to the study area was used to correlate the resistivity value obtained in order to arrive at the interpretation.

The study reveals the presence of subsurface contact between the two rocks, with chad formation laying uncomformably on the basement rock. The thickness of the uncomformity ranges from 0.993m to 26.930m. Geoelectric map was obtained using the resistivity of the first layer of all the VES points, the geoelectric boundary between the two rock formations and laterite was clearly delineated on the map.

Considering the pore volume and permeability of sand lithology, VES A9, A10 and B6 with the highest thickness of sand lithology of 26.66m, 26.93m and 18.42m respectively are the best positions to drill a productive borehole which will be an advantage to Kakara Community which

has no pipe borne water, the study is also useful in siting engineering structures as sand and clay has very low load bearing capacity.

TABLE OF CONTENTS **PAGE**

CHAPTER FIVE: Discussion

CHAPTER SIX: Conclusion and Recommendation

LIST OF TABLES

LIST OF FIGURES

LIST OF PLATE

LIST OF APPENDICES

ABBREVIATIONS AND SYMBOLS

D.C.	Direct Current
VES	Vertical Electrical Sounding
IDC	Industrial Development Centre
m	Metre
N	North
S	South
K	Geometric Factor
V	Electrical Potential
MN	Potential Electrode Separation
AB	Current Electrode Separation
ABU	Ahmadu Bello University, Zaria
ρ	Resistivity
Ω	ohm
ρ_a	apparent resistivity
σ	conductivity

CHAPTER ONE

Introduction

1.1 *General statement*

Surface electrical resistivity survey is based on the principle that the distribution of electrical potential in the ground in the vicinity of an electrode current array depends on the electrical resistivity distribution of the surrounding soil and rocks. The usual practice in the field is to inject a direct current through two electrodes, implanted in the ground and to measure the potential difference between the two other electrodes.

Mapping a transition zone between the basement complex rock and sedimentary rock can be difficult especially if there is absence of outcrops or any rock section exposure (Bayewu, 2011). However, in Kakara village the presence of quarry sites and erosion by seasonal rivers have helped in exposing the subsurface lithologies thereby giving clue about the nature of the transition zone and also how to position the sounding profiles so as to get the best subsurface picture of the transition boundary.

Some authors in Nigeria have used other Geophysical methods such as gravity and aeromagnetics (Bayewu, 2011) in delineating such Geological boundary. Electrical resistivity method can also be used to delineate the boundary between these rocks and is less costly and more environmental friendly. The resistivity parameter is extremely sensitive to rock texture, pore volumes, metallic mineral, change in clay content and weathered materials.

The objective of the present work is to evaluate the applicability of electrical resistivity sounding (VES) in delineating a transition zone between the basement rock and sedimentary

rock. The study area is Kakara village, Gezawa L.G.A., Kano state (Fig. 1.1) which is a transition area between basement older granite (undifferentiated) of Precambrian age and sedimentary rock of Alluvium Chad basin of recent to Pleistocene age.

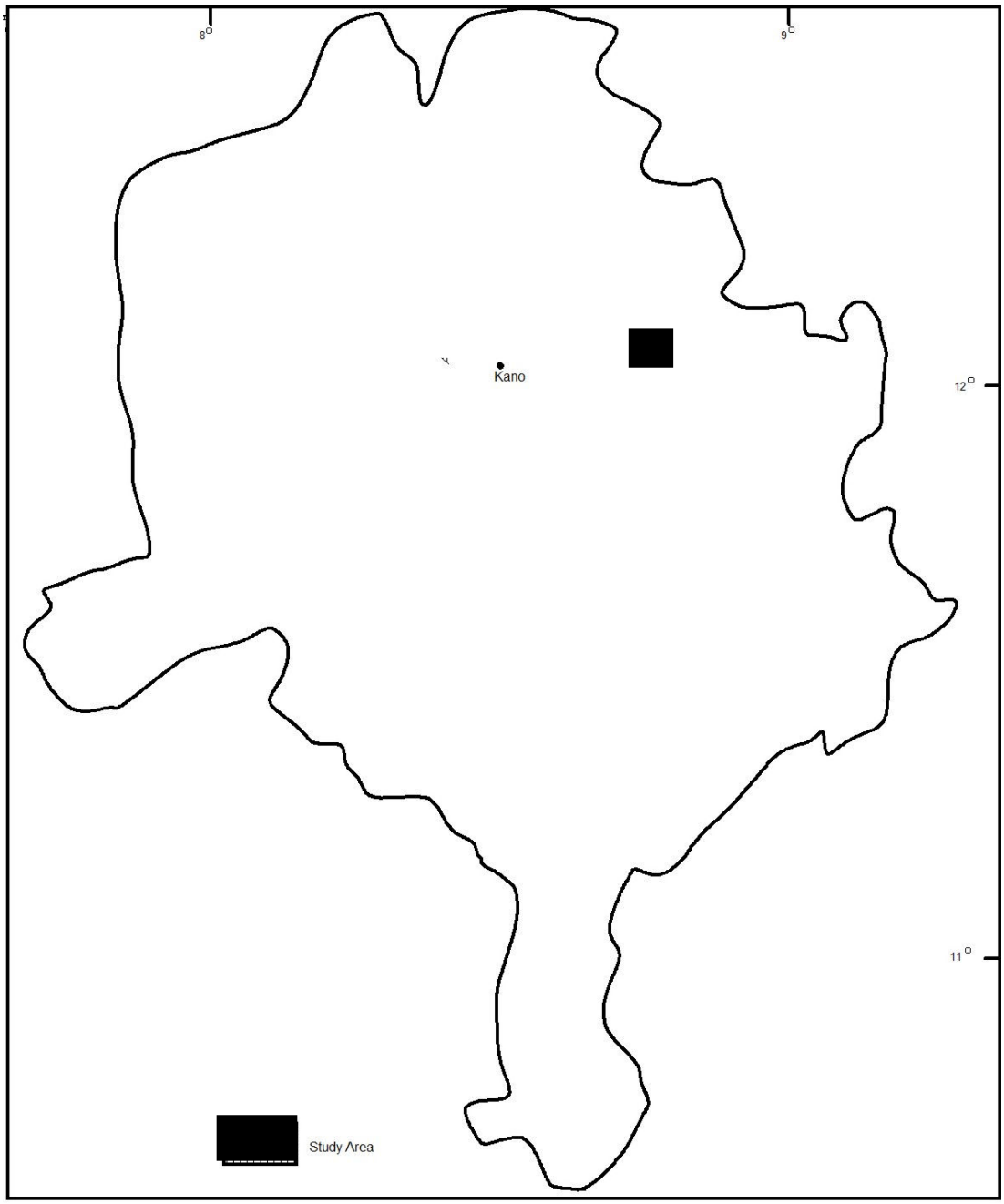

Figure. 1.1 Map of Kano state showing the study area

1.2 *Justification of the Study*

The study of geological structures is of prime importance in economic geology as geological boundary can serve as trap for accumulation and concentration of fluids such as petroleum, natural gas and water.

It is also very critical in civil engineering as physical and mechanical properties of natural rocks affect the stability of human engineered structures such as dams, buildings and road construction. However detailed study of geological structure gives clue on the geological history of an area.

1.3 *Location of the Study Area*

The area under study, Kakara village in Gezawa, Kano is located approximately between latitude 12.0129^0N and 12.0379^0N and between longitude 8.6313^0E and 8.6555^0E, it is along Gumel - Kano road Fig. 1.2. The terrain is relatively flat and the area can be accessed by motorable road.

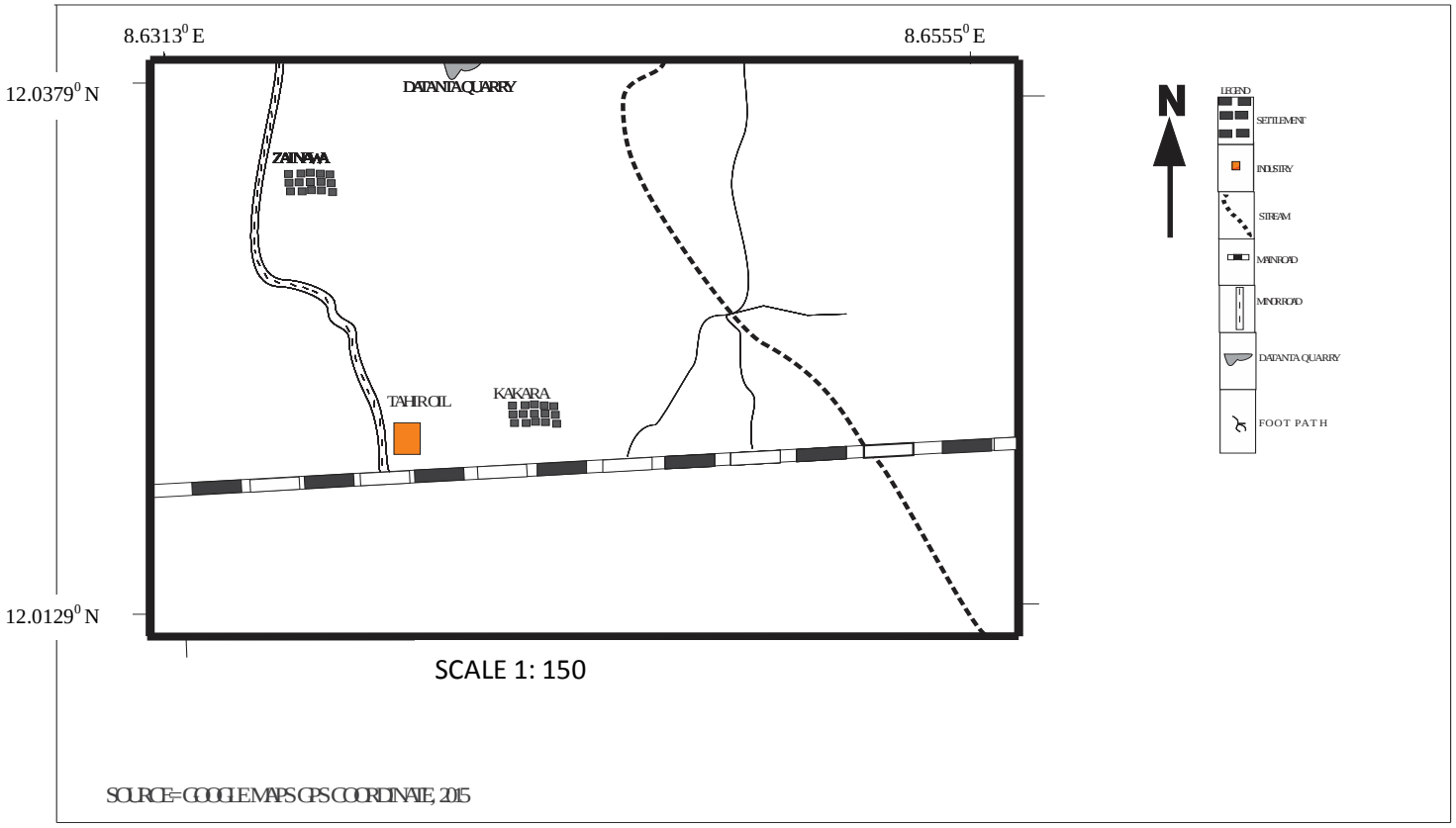

Figure 1.2 Map of the showing the study area, Kakara Village (source, Google image, 2015)

1.*4 Climate, Relief, Vegetation and Economic Activity of the study area.*

The study area, Kakara village in Gezawa Local Government Area, Kano state is in the tropical wet and dry climatic zone, characterized by strong seasonal rainfall and temperature distribution. The Climatic condition is controlled by two air masses, the maritime tropical air mass and the continental tropical air mass (Olugbenga, 2009). . When the maritime tropical air mass is prevailing, the Kakara area experiences a rainy season, while the continental tropical air mass controls the dry season with its cold, dry and dusty air which occasionally limits visibility and reduces solar radiation (Olugbenga, 2009). Daily maximum temperature shows a minor one in August (29^0C) and major peak in April (39^0C). The rainy season has a short duration and it is followed by 5-6 months of dry season. The rainy season appears to run from May to September while the dry season normally runs from October to April. The prevailing vegetation of tall grass and big trees is of economic importance during both the wet and dry seasons in the study area. About 95% of the Kakara village population is engaged in peasant farming, producing both food and cash crops such as millet, groundnut, soya beans, corn and e.t.c.

1.5 *Previous work in the study area*

The area under study lacks any detailed geophysical investigation. Most geophysical works carried out around this area are regional in nature or localized to some specific areas which are near to the study area. One of these is geophysical, geological and boreholes drilling carried out by Kano Agricultural and Rural Development Agency (KNARDA) around the area and beyound (KNARDA, 1989) and borehole drilling carried out by a Kano based company Tahir Water at Danzaki village near the study area (Tahir, 2003) Fig. 1.3 shows the borehole log of Tahir, 2003. They all suggest the presence of basement complex and sedimentary rock transition boundary.

Some work carried out by a company based in Kano Water Resources Engineering Construction Agency (WRECA) from Sauna in Kano metropolis up to Gumel in Jigawa State produced a regional geological cross section of the area and confirmed that the depth to basement was increasing from Sauna Quarters in the metropolis towards Gabasawa town eastwards.

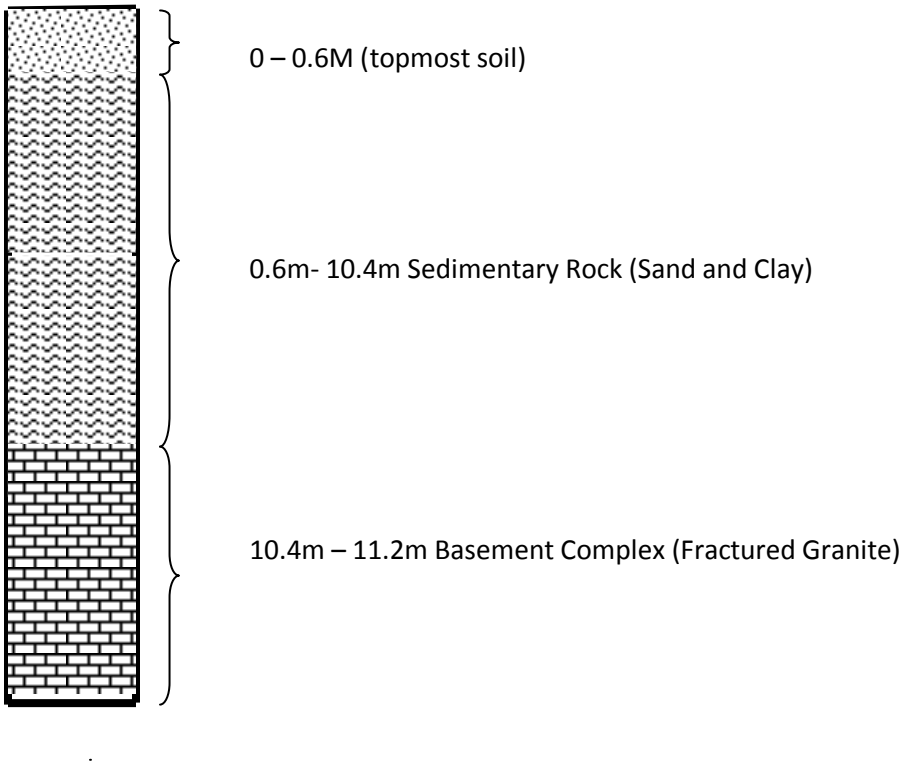

Figure. 1.3 Borehole log data drilled near the study area. (Tahir, 2003)

1.6 *Aim and Objectives of the Present Study*

The primary aim of this study is to investigate the transition boundary between the basement complex of northern Nigeria and sedimentary rock of Chad formation around Kakara village in Gezawa local government, Kano state. The objectives set to achieve this aim are:-

1. To carry out Geological mapping of the study area
2. To use the resistivity contrast and interpret various lithology at each point
3. To produce a cross section along the profile.
4 To produce Geoelectric map of the area based on the resistivity of first layer in the sequence.

Chapter Two

General geology

2.1 Introduction

Rocks of Northern Nigeria basement complex underline over 70% of Kano environs (KNARDA 1989). The basement Complex comprises three groups of rocks namely, migmatites and (high grade) gneisses derived from Birrimain sedimentary rocks through high grade metamorphism and granitization; the Younger Metasediments of Upper Proterozoic age which are low grade metamorphic rocks that were folded along with the migmatite and gneisses during the Pan-African orogeny; and the Older Granite series which were intruded during the Pan-African orogeny (McCurry, 1976). In the study area, Hazell et al., (1988) also report the occurrence of rocks of the Younger Granites series (Falconer, 1911). Also chad formation sediments are found in the north-eastern part of the state where unconsolidated aeolian sand form a drift plain, the rocks are fresh water sediments of lacustive and fluviatile clays, sandy clay and silts with bed lenses of sand and gravel at various levels fig. 2.1 (KNARDA 1989).

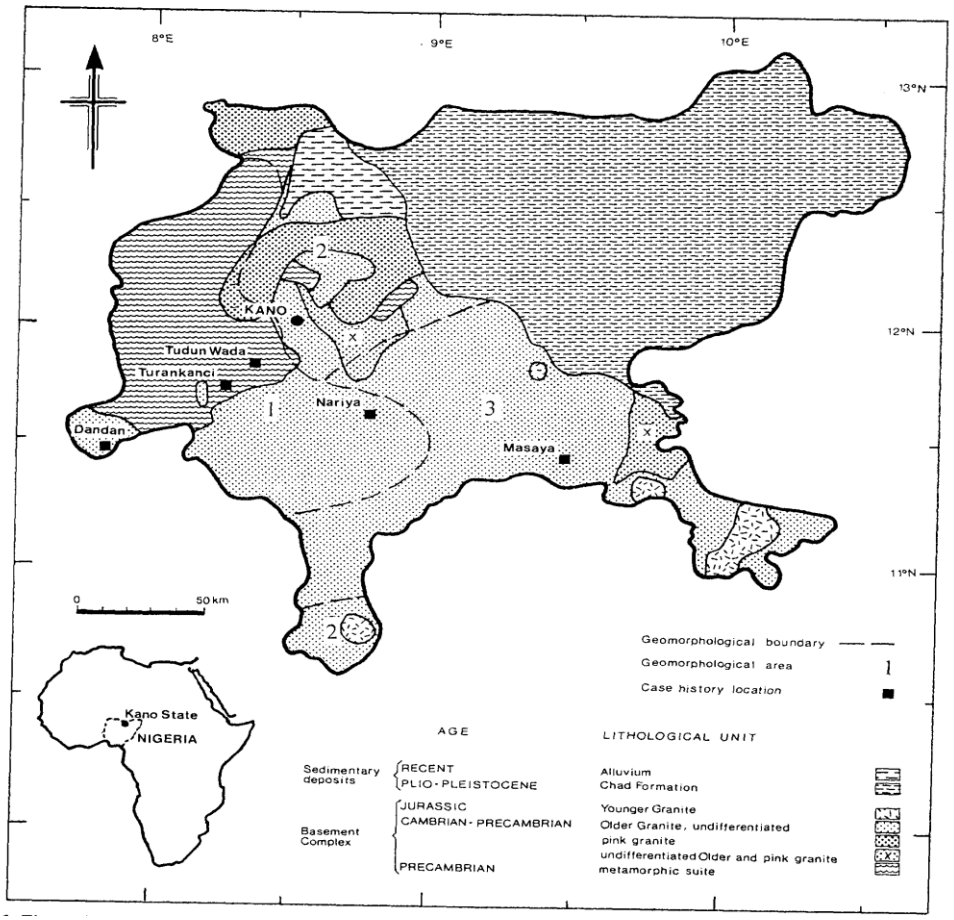

Figure. 2.1 Geological map of Kano and Jigawa State (KNARDA, 1989).

2.2 Older Metasediments

These rocks are believed to be Birrimian (>100 million year) in age and rock types include gneisses which have suffered at least two episodes of tectno-matamorphic deformation resulting in widespread occurrences of migmatitic and granitic gneisses (McCurry, 1976). They occupy isoclinal belts within the crystalline rocks with a N-S trending. Hence, it is overlain by igneous and metamorphic rocks.

2.3 Younger Metasediments

The younger metasediments are found in a well defined belt around the north- west and south-west of Nigeria. They are Katanga in age and believed to have been deposited on the originally granitic basement around 1800 million years ago. They were then folded during the Pan-African thermo tectonic events. They occurred as gold bearing quartzites in Ilorin.

2.4 Older Granites

They are believed to have intruded the Nigerian Basement Complex during the Eburnean and lower Cambrian ages. The Eburnean granites are fine grained granites that represent a group of minor discordant intrusions of small aerial extent, occurring as dykes and irregular bodies.

The group includes biotite and muscovite granite and adamebites. They are pale brown equigranular and usually foliated. According to Ogunmola *et al*. (2008), the Older Granite Series include rocks intruded during the Pan-African orogenic cycle. The earliest rocks appear to be basic and intermediate intrusives represented by small, irregular bodies of quartz and pyroxene diorite and gabbro. Granitisation on an extensive scale profoundly modified earlier rocks and resulted in widespread migmatites and granitic rocks. This granitisation culminated in the intrusion of a diverse and widespread suite of syn-to late-tectonic granites, granodiorites and syenites. Older granite rocks occur intricately associated with the Migmatite-Gneiss Complex and the Schist Belt into which they generally intruded (Obaje. 2009). They therefore, occur in

most places where rocks of the Migmatite-Gneiss or of the Schist Belt occur. They are found around Wusasa (Zaria), Abuja, Bauchi, Akwanga, Ado-Ekiti and Obudu area.

2.5 The Younger Granite

The Younger Granite ware first defined by Falconer (1911). He describe them as cross cutting alkali granites containing riekibite or biotite characterised by chilled margins against their country rock, he noted their undeformed post tectonic character, contrasting them with the foliated calc-alkaline Older Granite of basement, he recognised that younger granite are source of mineralization in Jos and Riruwai in Kano state.

There is variation in granite texture and composition usually occurs as abrupt changes at igneous contacts rather than transitions within a single body. Many complexes consist of a series of distinct intrusions often having a concerntric arrangement, each intrusion often having a concentric arrangement, each intrusion having characteristic petrographic features (Mac Kay, 1952).

The Younger Granite series or ring complexes that occurred during the time of Mesozoic (Jurassic) are faund in Northern Nigeria to have intruded the Precambrian basement rock. They are confined to zone stretching north-south of the Jos plateau and extend to the Niger Republic with their ages progressively decreasing from Niger Republic towards Nigeria with the youngest rocks found at the southern end of the ring complex. The major tectonic event that took place in

the Jos plateau around the Jurassic period resulted in the emplacement of the younger granites and associated rocks assemblage (Grant,1969) outcrop occur as large masses and sometimes as ring dyke. Member include rhyolite, gabbros and syenites.

2.6 Chad formation

The formation is a variable sequence that includes all quaternary sediments of lacustrine origin underlying the surface deposits of vast area (about 15,000km2) in Kano, Jigawa, Borno, Yobe and some part of Bauchi. The formation varies lithologically both laterally and vertically toward the centre of the basin, lacustrine clay are predominant in the sequence but near the margins fluviatile sand, grits, gravels become important (Barber, 1965).

The dating of chad formation is based on vertebrate remains of lower Pleistocene age and diatoms which are not older than the Pleistocene (Barber and Jones, 1960). In Nigeria a considerable thickness of chad Formation below these fossil bearing horizons in known, thus suggesting that the chad formation may also include deposits of Pliocene age (Barber, 1965).

2.7 Geological setting of the study area

The study area lies within a transition zone between the chad formation and basement complex rocks in the eastern part of Kano. The sedimentary part of the study area is located within the Chad formation in Chad basin, the lithostatigraphy of this formation is an argillatious sequence in which impersistance arenecous sequence formed, clay sequences are formed as a result of deposition under less turbulent condition away from the shore of the lake, the sandy sediment are thought to have been laid down as lake margin deposits or as alluvial fans and deltas (Barber, 1965)

The basement complex is composed mainly of older granite and granodiorite. Biotite granite is an acid igneous rock with biotite mineral while granodiorite has a composition which is intermediate between a diorite and granite.

Joint and fractures in the basement complex rocks are better developed in granites and quartzite and less in gneiss and migmatites, and it rarely extends to a depth greater than 90 meters (Ahmed, 1987)

There is exposure of basement rock in outcrops and quarry site in the study area and the sedimentary Chad formation on the surface as shown in as part of the study area has been excavated by seasonal rivers and in quarry activities thereby exposing the lithological section of both the basement complex and sedimentary rocks.

CHAPTER THREE

Principles and Theory of the Method Used

3.*1* *Principle of Resistivity Method*

The principle of the electrical resistivity method is the measurement of an earth resistance by passing low frequency current (d.c. preferably) into the ground through two metal stakes or electrodes and measuring the potential difference resulting across another two electrodes. If the distance between the four electrodes is known then, this together with the current and potential difference measurements may be used to calculate a 'resistivity' value of the earth (Thomas, 1986). All resistivity methods employ an artificial source of current which is introduced into the ground through point electrodes or long line contacts. The latter arrangement is rarely used nowadays. The procedure is to measure potentials at other

electrodes in the vicinity of the current flow. Because the current is measured as well, it is possible to determine an effective or apparent resistivity of the subsurface. In this regard the resistivity technique is superior at least theoretically to all the other electrical methods because quantitative results are obtained by using a controlled source of specific dimension (Telford et al., 1990).

The resistivity of rocks usually depends upon the amount of groundwater present and upon the amount of salt dissolved in it. It decreases by the presence of many ore minerals and by high temperature (Alan et al., 2000). Conduction of electricity through rocks is of three types; electronic conduction which occurs when the mineral grains are electrically conductive as with minerals such as pyrite, and magnetite while most common minerals such as quartz, feldspar and calcite, are not electrically conductive, in this case conduction is through ions called ionic conduction and the third type of current conduction is dielectric conduction which occur in poor conductors or insulators having very few charge carriers or even none. The main uses of resistivity surveying are for mapping the presence of rocks of differing porosities, particularly in connection with hydrogeology for detecting aquifers and contamination, and for mineral prospecting (Telford et al., 1990). But other uses include archaeological surveying and investigating saline and other types of pollution.

3.2 *Theory of D.C. Resistivity Method*

D.C. resistivity (electrical resistivity) technique is used to measure earth resistivity by driving a direct current (D.C.) signal into the ground and measuring on the earth's surface the resulting potentials created. For direct current flowing in a subsurface homogeneous isotropic medium, the potential at a single point electrode can be obtained using Ohm's law.

$$E = \rho J \qquad (2.1)$$

where E = The magnitude of the electric field intensity

ρ = The resistivity of the medium, and

J = The magnitude of the current density

Also, consider the divergence condition which states that all the current flowing into a chunk of material must leave from the other side provided there is no current source or sink within the chunk. The divergence of the current density vector must be zero everywhere except at the current source, and this is the principle of charge conservation, hence

$$\nabla . J = 0 \qquad (2.2)$$

From equation (2.1)

$$J = \sigma E$$

where E is the gradient of scalar potential u and

σ is the conductivity

Hence $E = -\nabla u$

Therefore,

$$J = -\sigma \nabla u \qquad (2.3)$$

Substituting equation (2.3) in (2.2) and considering an isotropic homogeneous medium, implies σ is constant, hence,

$$\nabla^2 u = 0 \qquad (2.4)$$

Equation (2.4) is called Laplace's equation; for this equation to hold it must satisfy some relevant boundary conditions.

In spherical polar coordinates, Laplace's equation is

$$\frac{1}{r^2}\frac{\partial}{\partial r}\left(r^2\frac{\partial u}{\partial r}\right) + \frac{1}{r^2 \sin\theta}\frac{\partial}{\partial \theta}\left(\sin\theta\frac{\partial u}{\partial \theta}\right) + \frac{1}{r^2 \sin^2\theta}\frac{\partial^2 u}{\partial \emptyset^2} = 0 \qquad (2.5)$$

r, θ,Ø are related to Cartesian coordinates (x, y, z) where r is the distance, θ is the radial polar coordinate and Ø is the azimuth angle. Now if only a single point current source is considered to pass current into a finite homogeneous medium, there is complete symmetry of the current flow with respect to θ and Ø directions and the derivatives with respect to these directions are zero. Hence, equation (2.5) will be a function of r only

$$\frac{1}{r^2}\frac{\partial}{\partial r}\left(r^2\frac{\partial u}{\partial r}\right) = 0 \quad \text{and} \quad \text{since } r \neq 0 \text{ then, } \frac{d}{dr}\left(r^2\frac{\partial u}{\partial r}\right) = 0$$

This on integration gives,

$$r^2\frac{du}{dr} = a \qquad (2.6)$$

integrating again:

$$\frac{du}{dr} = \frac{a}{r^2}$$

$$du = a\frac{dr}{r^2}$$

$$\int du = a\int \frac{dr}{r^2}$$

$$\int du = a \int r^{-2} dr$$

u = - a r^{-1} + b

$$u = -\frac{a}{r} + b \qquad (2.7)$$

a and b are constants and r is the distance from the point current electrode to the electric potential point.

Since u = 0 when

r $\rightarrow$ ∞, then b = 0. That is, $u = -\frac{a}{r}$ (2.8)

Now for a point current electrode at the surface of a homogeneous isotropic medium the current flows through a hemispherical surface in the lower medium then,

$$I = 2\pi r^2 J \qquad (2.9)$$

From equation (2.3)

$J = -\sigma \frac{du}{dr}$ substituting for J in the equation (2.9) gives;

$I = -2\pi r^2 \sigma \frac{du}{dr}$ where $r^2 \frac{du}{dr} = a$ (from equation 2.6). Thus,

$I = -2\pi\sigma a = -\frac{2\pi a}{\rho}$

therefore, $a = -\frac{I\rho}{2\pi}$ hence, from equation (2.8)

$u = \frac{I\rho}{2\pi r}$ (2.10a) or $\rho = 2\pi r \left(\frac{U}{I}\right)$ (2.10b)

In a case of several point current sources the total potential U at an observation point M is the algebraic sum of potential contribution from each current source considered independently. Thus, for n- point current sources equation (2.10a) becomes;

$$u_M = \frac{\rho}{2\pi}\left(\frac{I_1}{r_1} + \frac{I_2}{r_2} + \frac{I_3}{r_3} + \ldots + \frac{I_n}{r_n}\right) \qquad (2.11)$$

where I_1 is the current source one and r_1 is the distance from the point current source to the observation point M.

Now consider two point current electrodes A and B at the surface of homogeneous earth with current output I. Since the distance between the current electrodes is finite, both electrodes will contribute to the potential at any nearby surface point. Assuming that the potential gradient associated with this current is measured across two electrodes M and N on the surface, then the electric potential at M will be;

$$u_m = \frac{I\rho}{2\pi}\left(\frac{1}{r_1} - \frac{1}{r_2}\right) \qquad (2.12)$$

since the current at the two electrodes are equal and opposite in direction, that is, one current is the source and the other is the sink. Similarly the potential at N is

$$u_n = \frac{I\rho}{2\pi}\left(\frac{1}{r_3} - \frac{1}{r_4}\right) \qquad (2.13)$$

where r_1 is the distance between the current electrode A and potential electrode M and r_2 is the distance between the same potential electrode and the current electrode B. r_3 is the distance between the current electrode A and potential electrode N, and r_4 is the distance between the same potential electrode to the current electrode B, as shown in fig 3.1.

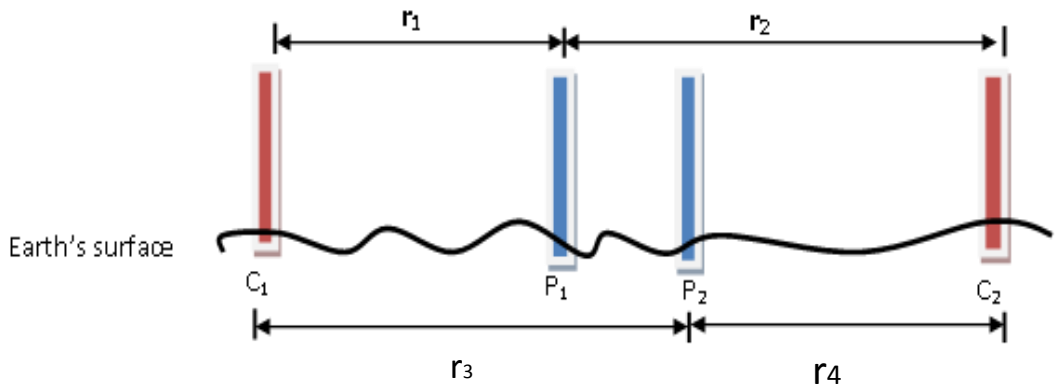

Figure 3.1 the general four-electrode configuration

From equations (2.12) and (2.13), the potential difference Δu measured across M and N electrodes is $\Delta u = u_m - u_n$

$$= \frac{I\rho}{2\pi}\left\{\left(\frac{1}{r_1} - \frac{1}{r_2}\right) - \left(\frac{1}{r_3} - \frac{1}{r_4}\right)\right\} \qquad (2.14)$$

This electrode arrangement is called the general four - electrode spread, corresponding to the many four - electrode spreads normally used in resistivity fieldwork (Telford et al., 1990). Schlumberger electrode arrangement will be adopted in this present study. From the above equation the apparent resistivity for non – uniform earth can be expressed as,

$$\rho_a = \frac{\Delta u}{I}\left[\frac{2\pi}{\left(\frac{1}{r_1} - \frac{1}{r_2}\right) - \left(\frac{1}{r_3} - \frac{1}{r_4}\right)}\right] \qquad (2.15)$$

the term inside the square bracket is called the geometric factor denoted by letter K. The geometric factor depends on the type of electrode configuration used. The geometric factor for Schlumberger array in symmetrical arrangement is given as:

$$K = \pi\left(\frac{L^2}{2b} - \frac{b}{2}\right) \qquad (2.16)$$

where L is the half current electrode separation (AB/2), and 2b is the separation of the potential electrodes (MN).

3.3 *Electrode Configuration*

Many different electrode spreads have been used in the past but only few are still in use. These include; Schlumberger array, Wenner array and double – dipole array. However, the most widely and commonly used are Schlumberger array and Wenner array.

(1) Schlumberger Array

In Schlumberger array the current and potential pairs of electrodes have a common mid- point (symmetrically arrangement). All the four electrodes are arranged collinearly, the current electrodes are usually much further apart than the potential electrode (Fig.3.2). The smallest current- potential electrode distance is always much greater than the distance between the two potential electrodes (Telford et al., 1990).

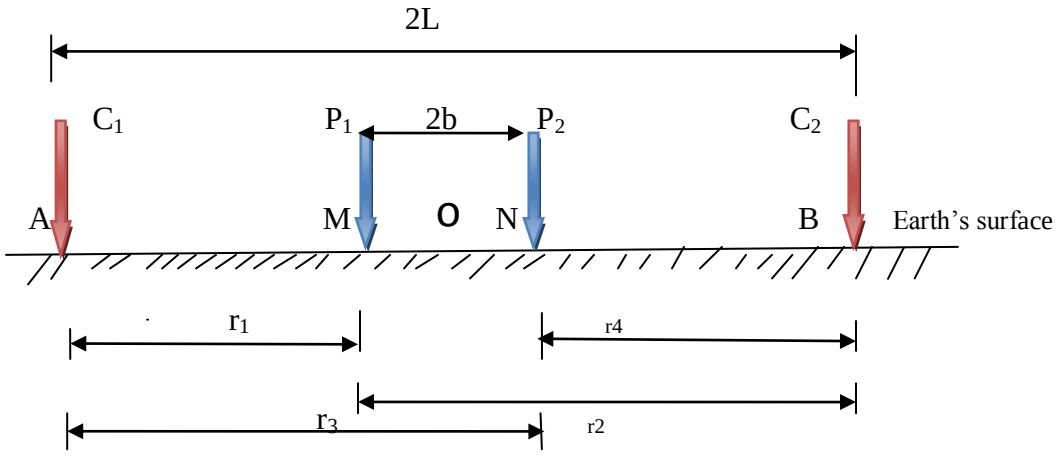

Figure 3.2 Schematic diagram of Schlumberger symmetrical Array.

In depth probing the potential electrodes are fixed while the current electrode separation is increased symmetrically about the center 0 of the spread. However, when expansion of the current electrodes causes the potential difference to become so small that it cannot be measured precisely, the potential electrodes are moved further apart, while keeping the current electrodes fixed, and then further readings are taken by expanding the current electrodes using the new potential electrode positions. The apparent resistivity is plotted against electrode spacing L on log- log scale.

(2) ***Wenner Array***

In Wenner configuration, the current and potential pairs of electrodes have a common mid-point, and the distance between adjacent electrodes is equal. Thus, $r_1 = r_4 = a$ and $r_2 = r_3 = 2a$ and a is called the array spacing. For depth exploration the electrode (or array) spacing 'a' is increased in step. The apparent resistivity is plotted against electrode spacing on a log- log scale. For lateral exploration or mapping, the array spacing is fixed and all the electrodes are moved along a line profile, then along another line and so on. The apparent resistivity for each array position is plotted against the centre of the spread (Telford et al., 1990). Fig. 3.3 shows a schematic arrangement of Wenner array.

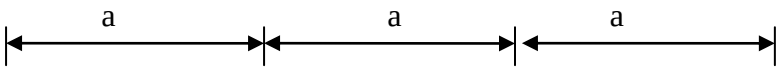

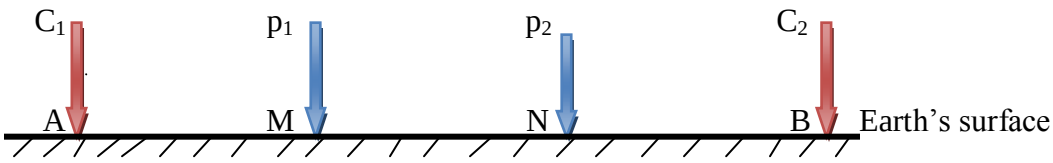

Figure 3.3 A Schematic Diagram of Wenner array

3.4 *Vertical Electrical Sounding (VES)*

Vertical Electrical Sounding (VES) is a geoelectric resistivity method to measure vertical variation of electrical resistivity (Kelly, 1993). It is well known that resistivity methods can be successfully employed in lithological investigations where there is a good electrical resistivity contrast between the various formations. Vertical Electrical Sounding (VES) also called depth sounding or sometimes electrical drilling is used when the subsurface approximates to a series of horizontal layers each with uniform but different resistivity. The goal is to observe the variation of resistivity with depth. Schlumberger configuration is most commonly used for VES. The mid-point of the array is kept fixed while the distance between the current electrodes is progressively increased. This causes the current lines to penetrate to ever greater depth depending on the vertical distribution of conductivity. A typical VES and the current distribution is illustrated in fig. 3.4 .

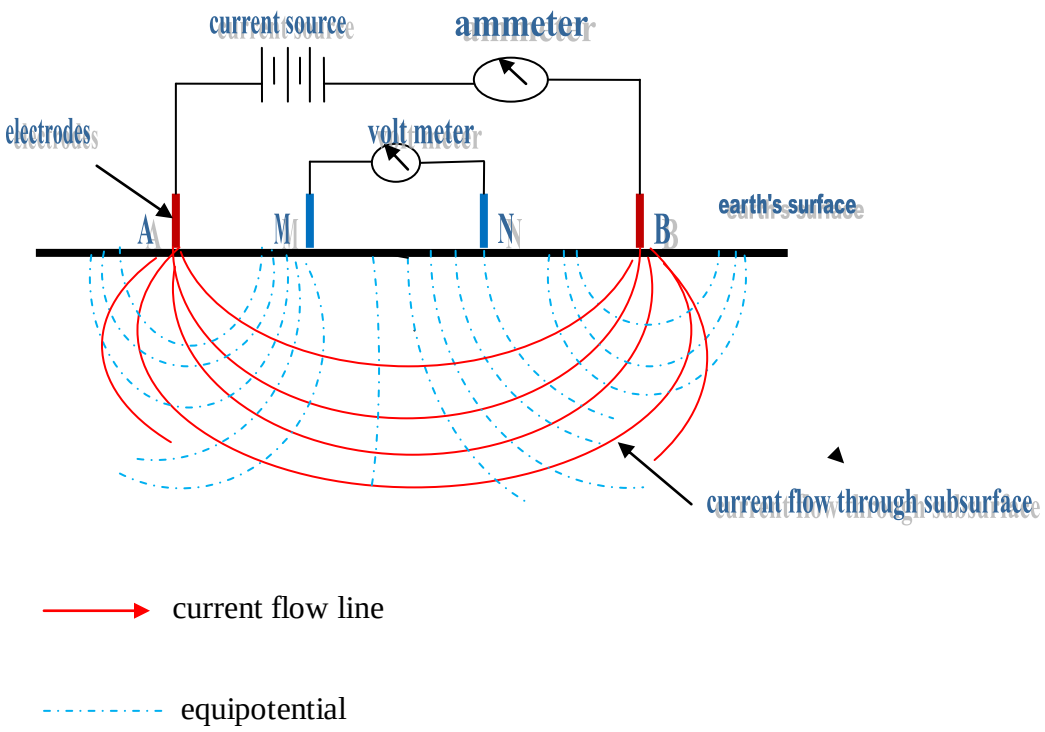

Figure 3.4 Schematic illustration of Basic Concept of Electrical Resistivity Measurement.

The characteristic curves can be computed for the interpretation of structures with multiple horizontal layers. Modern VES analysis has advantage of the flexibility offered by small computers with graphic outputs on which the apparent resistivity curves can be visually assessed. Interpretation with computer software is also adopted for this study so as to enhance good interpretation.

The apparent resistivity curve for a three- layer structure generally has one of four typical shapes, determined by the vertical sequence of resistivity in the layers. The type K curve rises to a maximum then decreases, indicating that the intermediate layer has higher resistivity than the top and bottom layers. The type H curve shows the opposite effect; it falls to a minimum then

increase, again due to an intermediate layer that is a better conductor than the top and bottom layers. The type A curve may show some changes of gradient but the apparent resistivity generally increases continuously with increasing electrode separation, indicating that the true resistivity increase, with depth from layer to layer. The type Q curve exhibits the opposite effect; it decreases continuously along with a progressive decrease of resistivity with depth (Lowrie, 1997).

CHAPTER FOUR

Methodology and Field Procedure

4.1 Geological mapping

The geological mapping of the study area was conducted along footpath, so as have bases for correlation with the exposed rocks observed during the mapping and electrical resistivity sounding results for accurate interpretation.

During the mapping rocks where observed on hand specimen. Basement rocks where identified based on textural characteristics and colour while sedimentary chad formation was identified based on lithology observed from erosion sites and exposed sections along river bank.

The geological mapping shows that the study area was characterised by two rock types the basement complex composed of granite and sedimentary rock with sequences of sand and clay. The geological boundary has been delineated clearly in the mapping as shown in Fig. 4.1

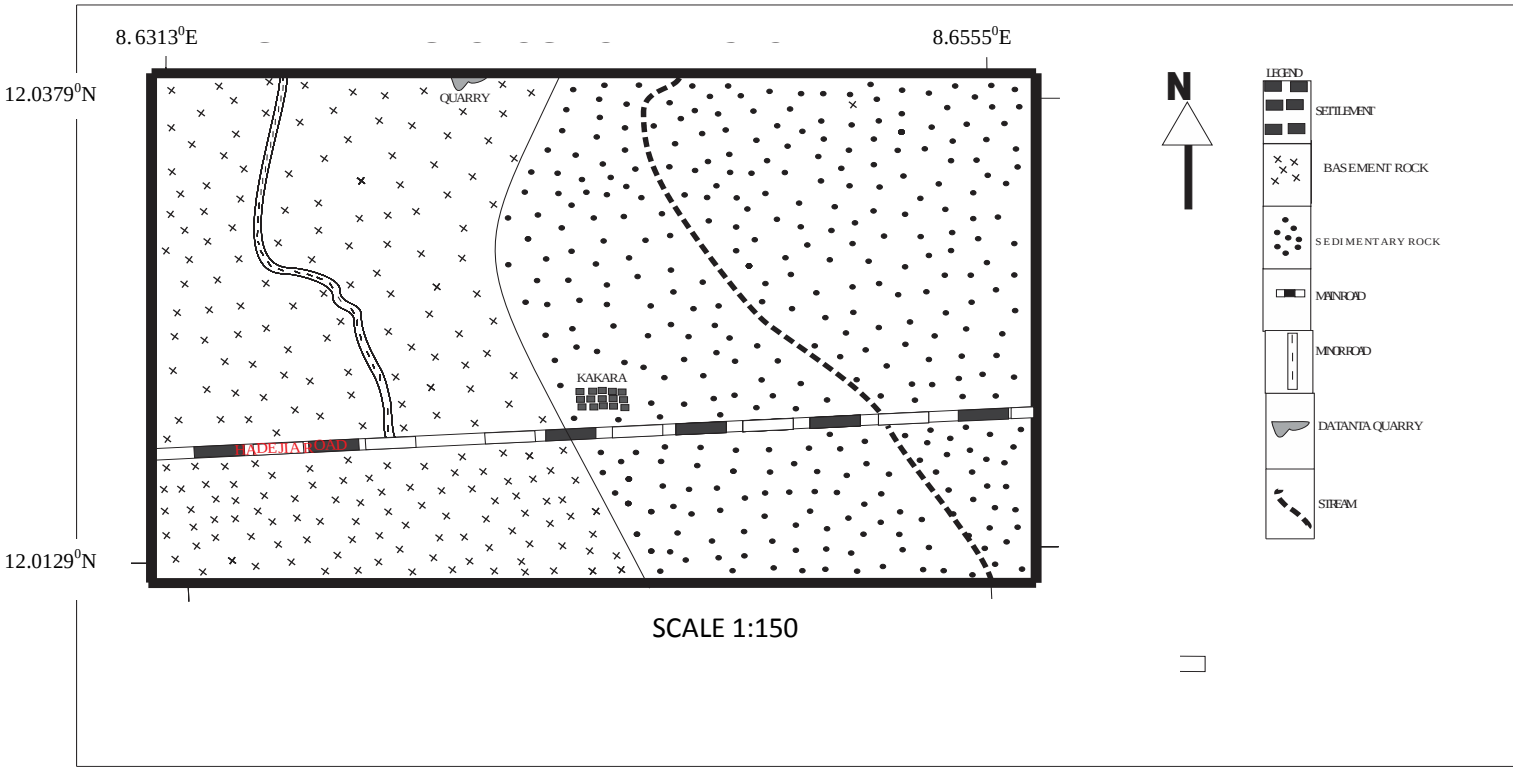

Figure 4.1 Geological map of Kakara village.

4.2 *Data Collection*

Vertical Electrical Sounding (VES) D.C resistivity method was carried out in the study area using Schlumberger array along two profiles, AA and BB with a total of 24 Vertical Electrical Soundings (VES) 12 sounding points on each profile, at an average of 100m apart at locations within the study area as illustrated in fig. 4.2.

The choice of array and its dimension largely is based upon the target size, depth and resistivity contrast within the surroundings. For this present study Schlumberger array was adopted because of the following advantages;

1) The smaller separation of the potential electrode reduces noise due to ground current (from industrial and telluric sources) which may limit the useful depth of penetration.
2) The Schlumberger method has a greater penetration than the Wenner.
3) In general VES method with Schlumberger array assumes considerable importance because it can easily detect the presence of horizontal or gently dipping beds of different resistivity.

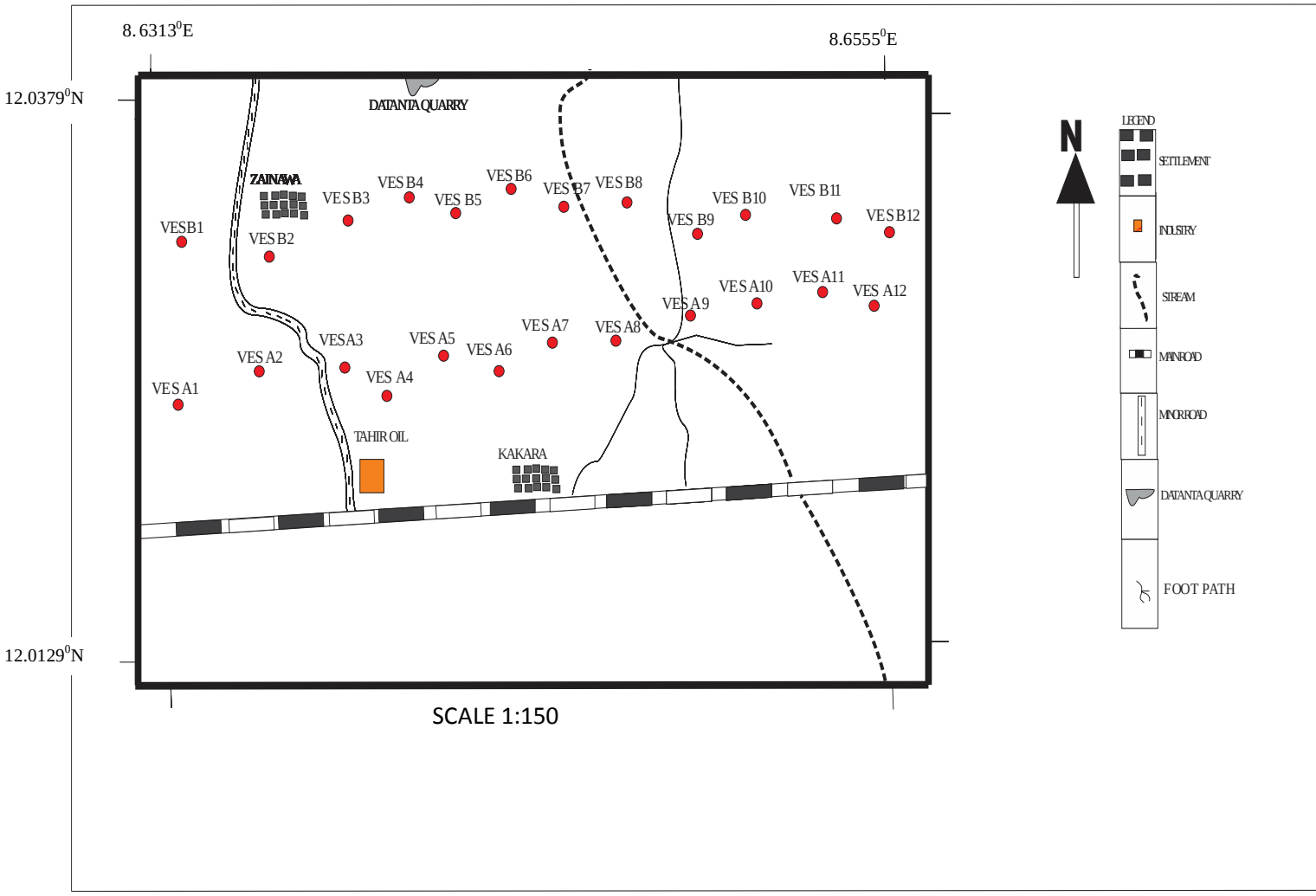

Fig 4.2 Basemap of the study area showing VES points.

4.3 *Instrumentation*

In this survey the instruments used for data collection are; Geopulse system and its accessories, magnetic compass, field hammer, cutlass, ranging pole, pegs, electrodes, cable and reel, measuring tape, global positioning system (GPS), and other accessories as shown in Plate I. The Geopulse system works when the operator presses the measure button; the micro processor runs

through checks the circuit and positions, the battery condition and usability of selected parameters. This check–up takes only one second and if necessary information comprising beeper signals and error codes tell the operator to check circuit or change parameter. When satisfied the micro processor automatically start the measurement cycle and after all the readings have been taken it puts the instrument in a standby mode with the resistivity displayed.

The Geopulse is composed of deep penetrating resistivity meter with an output for maximum current electrode separation (AB) of up to 2000 metres under favourable condition. The resistivity is calculated automatically that is ($\Delta V/I$) and displayed in digital form in kilo –ohms, ohms, or milli- ohms, up to a range of 0.5 milli- ohm to 1999 kilo- ohms, Booster which is optional, supplements the Geopulse in situation where the voltage and/or current needs to be increased. With the help of Booster, this range can be extended down to 0.02milli- ohms. However, in this survey no Booster has been used because the current and/or voltage is sufficient enough for the measurements.

Plate I. Geopulse system and its accessories

4.4 *Field Procedures*

Measurements were taken along two profiles 100m apart and station interval of 100m was used to establish various sounding points. Measurements were taken at each VES point by expanding the current electrodes symmetrically about the centre of the spread. The maximum exploration depth (also known as depth of penetration) of the AMNB method is ¼ to 1/3 of the maximum distance of AB (Frohlich et al., 1996). That is, the maximum measurement for AB = 70.0m the maximum depth probed is about 18.0m to 23.0m. This depth is considered enough to delineate the interface between the two rock types of interest. Measurements were taken from AB/2 = 1.5m, 2.0m, 3.0m, 4.5m, 7.0m, 10.0m, 15.0m, 20.0m, 30.0m, 45.0m, 60.0m to 70.0m. At a distance when the potential difference between the potential electrodes was too small for the

potential difference to be measured accurately, the potential electrodes spacing (MN) was also increased from 0.5m to 2.0m to obtain a measurable potential. Measurement then continued to next AB/2, using the new potential electrodes position, and then to the next, until to a distance of 100.0m, then the equipment was moved to the next VES point and repeated the same procedure until all the VES point are covered. Readings were taken on two profiles each consisting of twelve VES stations.

4.5 *Data processing*

The data collected were reduced using an equation below example is shown in table 4.1 the apparent resistivity were then plotted against their corresponding AB/2 values on log-log graph paper using computer software (IX1D). The half length of the current electrodes separation (AB/2) is plotted on the abscissa while the corresponding apparent resistivity is plotted on the ordinate. A typical example of such plots is shown for VES station A1 in Fig 4.3 and the interpreted result in table 4.2. The VES plots for other stations with their interpreted curves are shown in appendix 1. The computer software used (IX1D) is designed for Vertical Sounding, Electromagnetic and/or induced polarization data 1D interpretation.

$$\rho_a = \frac{\Delta u}{I}\left[\frac{2\pi}{\left(\frac{1}{r_1} - \frac{1}{r_2}\right) - \left(\frac{1}{r_3} - \frac{1}{r_4}\right)}\right]$$

ρ_a = apparent resistivity in ohm- metre.

The term inside the square bracket is called geometric factor denoted by letter K, for Schlumberger symmetrical array, the expression for K is given below.

K = $\pi\left(\frac{L^2}{2b} - \frac{b}{2}\right)$ where L is the half current electrode separation (AB/2), and 2b is the separation of the potential electrodes (MN).

Table 4.1: Typical resistivity data (VES A1)

S/N	L(m)	b(m)	K (m)	R(Ω)	APP. RES. (ohm-metre)
1	1.5	0.5	6.2832	490.000	3078.7680
2	2.0	0.5	11.7810	184.000	2167.7040
3	3.0	0.5	27.4889	60.900	1674.0764
4	4.5	0.5	62.8319	14.400	904.7794
5	7.0	0.5	153.1526	4.630	709.0965
6	10.0	0.5	313.3739	2.170	680.0214
7	15.0	2.0	173.5730	3.570	619.6556
8	20.0	2.0	311.0177	2.110	656.2473
9	30.0	2.0	703.7168	1.150	809.2743
10	45.0	2.0	1587.2897	0.578	917.4534
11	60.0	2.0	2824.2918	0.413	1166.4325
12	70.0	2.0	3845.3094	0.208	799.8244

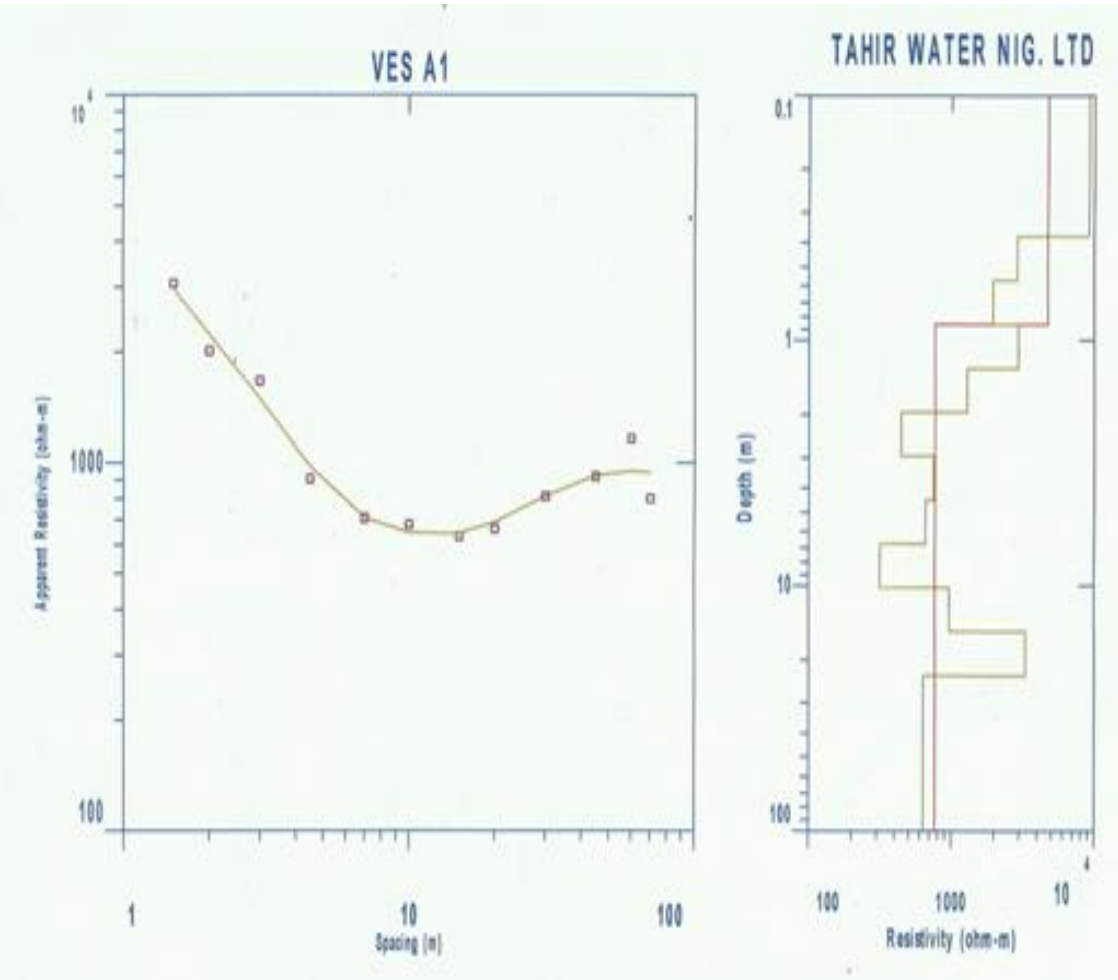

Figure 4.3 A typical resistivity curve and interpreted model for VES A1 station

Table 4.2 Interpretation of VES A1

STATION	SEQUENCE	RESISTIVITY (Ωm)	THICKNESS (m)	DEPTH (m)	LITHOLOGY
A1	1	4693	0.993	0.993	LATERITE
	2	767			FRACTURED BASEMENT

CHAPTER FIVE

DISCUSSION

5.1 *Interpretation*

Available geological controls such as borehole data, hand dug wells, exposed sections of the rock formations, geological mapping of the study area and resistivity values of earth materials compiled have been used in order to have a meaningful interpretation

Assumption has been made in the interpretation of Vertical Electrical Sounding (VES) data that: (a) the various geoelectric layers encountered are electrically homogeneous and isotropic. However, because of the existence of lateral variation in resistivity within a layer, possibility of error in interpretation is present.

(b) the principle of equivalence that is, non unique solution for a number of types of a typical three layer curve which are only distinguished by the resistivity value of their second layer in a relation to the value of either the first or third layer. Typical examples are type A (P1<P2<P3) and type H (P1>P2<P3) curves, where P1, P2 and P3 are the resistivity of first, second and third sequence in the lithology respectively.

5.2. *Result*

The data analysis for the Vertical Electrical Sounding (VES) was performed using computer software (IXID) as stated before. Borehole lithological logs near the area, exposed cross section

of rock formation in the area and hand dug wells around the area were considered in order to arrive at the resistivity values used for the interpretation of this present work and also resistivity values given by Telford et al. (1990) are considered table 5.1.

Table 5.1 Resistivity values adopted for this study. Source: Shemang (1990), Telford et al., (1990), Olugbenga (2009).

ROCK TYPE	RESISTIVITY VALUE (Ωm)
Fadama Loam	30 - 90
Clay, Sandy silt, Sandy clay,	100 - 200
Fresh Laterite	850 - 3000
Weathered Laterite	30 - 300
Weathered basement	20 - 300
Weathered basement (lateritic)	300 - 1500
Fractured basement	500 - 1000
Fresh basement	>1000

The results of the interpreted resistivity values for VES A1, A2, B1 and B2 stations are shown in Table 5.2 and 5.3. Results of the other VES points are shown in appendix 1.

Table 5.2 Interpreted model and lithology for VES A1 and A2 (Profile A)

PROFILE A

STATION	SEQUENCE	RESISTIVITY (Ωm)	THICKNESS (m)	DEPTH (m)	LITHOLOGY
	1	4693	0.993	0.993	LATERITE
A1	2	767			FRACTURED BASEMENT
	1	3386	0.225	0.225	LATERITE
	2	10	0.788	1.030	CLAY
A2	3	1458			FRESH BASEMENT

Table 5.3 Interpreted model and lithology for VES B1 and B2 (Profile B)

PROFILE B

STATION	SEQUENCE	RESISTIVITY (Ωm)	THICKNESS (m)	DEPTH (m)	LITHOLOGY
	1	485	25.483	25.483	FRACTURED BASEMENT
B1	2	921			FRESH BASEMENT
	1	366	3.480	3.480	FRACTURED BASEMENT
B2	2	2445			FRESH BASEMENT

5.3 Discussions *of result*

The iterated curves plotted along the two profiles A and B were used to produce the two geoelectric sections Figs. 5.1 and 5.2 with contact zone between the two rocks basement complex and sedimentary rock been clearly delineated .

Resistivity range of 1074Ὼm to 4692Ὼm is interpreted as laterite, 4Ὼm to 10Ὼm corresponds to clay and 25Ὼm to 92Ὼm corresponds to sand, which are part of lithological sequences of sedimentary chad formation. While resistivity range of 180Ὼm to 876Ὼm corresponds to

fractured granite and 1458Ώm to 68,161Ώm correspond fresh granite which is part of basement complex.

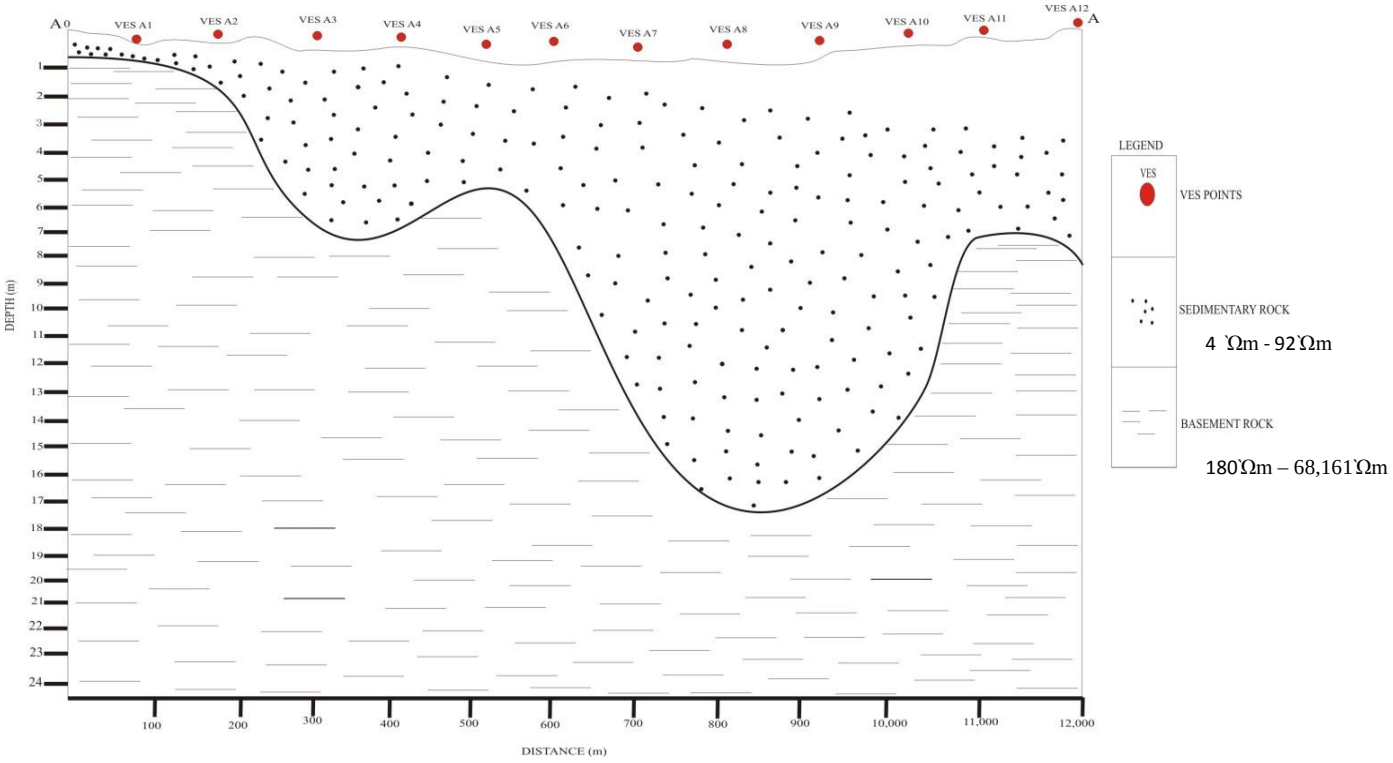

Figure 5.1 Geoelectric section beaneath VES A1 – A12

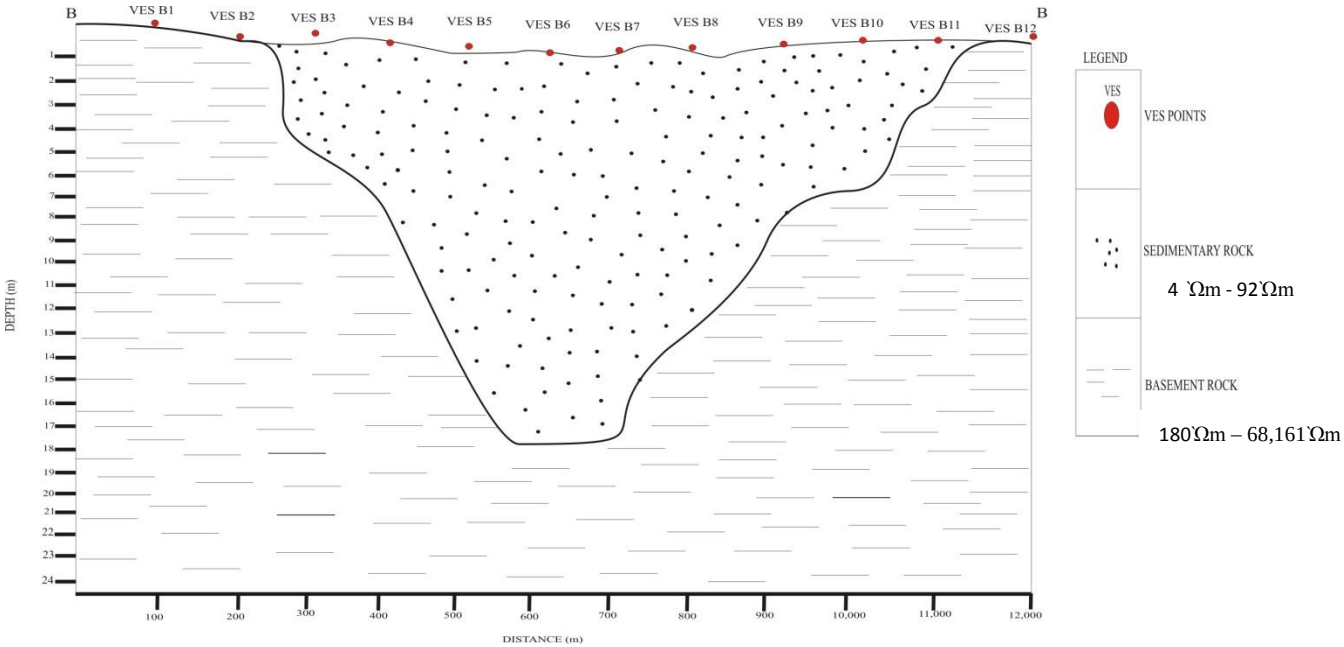

Figure 5.2 Geoelectric section beneath VES B1 – B12

The Geoelectric map was obtain using resistivity values of first layer in the sequence of all the 24 VES points. The boundary between the two rocks has been delineated basement complex has resistivity range of 180Ώm to 876Ώm, sedimentary with resistivity range of 25Ώm to 92Ώm and laterite having resistivity range of 1074Ώm to 4693Ώm Fig 5.3 and it shows considerable agreement with the Geological mapping of the area.

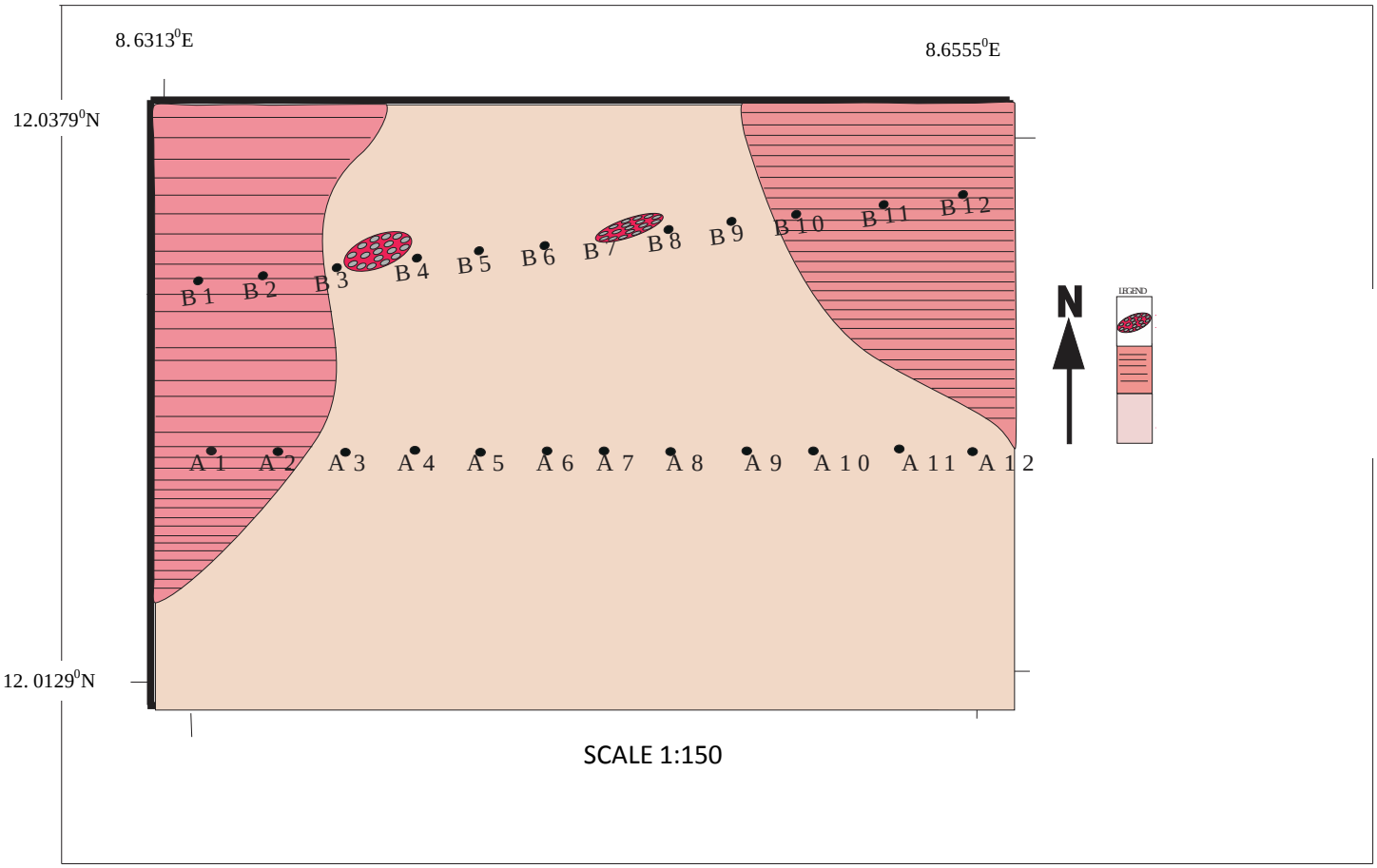

FIGURE 5.3 Geoelectric map of the study area

CHAPTER SIX

CONCLUSION AND RECOMMENDATION

6.1 *Conclusion*

Structurally according to the result the contact zone is a nonconformity that is the younger sedimentary rock unit laying on the older basement rock which suggests there was a long term of weathering and erosion which exposed the basement before it was finally buried by the sedimentary rock. The thickness of the sedimentary bed (sand and clay) is at its maximum of 26.93 metres and 18.23 metres in VES A10 and VES B6 respectively which can be a good source of underground water while it will not be a good site for building construction because sand and clay have very low load bearing capacity.

6.2 *Recommendations*

The study area has no detailed record of any geophysical investigation and the only borehole log available is not detailed enough, as a result the conclusion derived cannot be compared with any previous results. It is recommended that further geophysical and geological investigations employing other methods should be carried out in the study area. Also other Geophysical

methods such as seismic and gravity should be employed along the resistivity method because no single method can provide adequate and complete information about subsurface structures of an area. Secondly it is also recommended to extend the study coverage so as to see the extensive picture of the boundary.

REFERENCE

Ahmed, K. (1998). Water quality for Irrigation in Hadejia River Catchment, Arts and Social Science Reasearch, Vol. 1, pp119-129

Alan,E., Mussett, M. and Aftab, K.(2000). Looking into the earth. Cambridge University Press, United Kingdom.Pp 456-476.

Ariyo, O. and Gabriel, O. (2009). Role of electrical resistivity method for groundwater exploration in hard rock areas: a case study from Fidiwo/Ajebo area of south western Nigeria. Pacific Journal of Science and Technology, 10(1) : 483-486.

Baker, R.D. (1989). Depth of investigation of a generalized collinear 4- Electrode Array. Geophysics 54:1031-1037.

Barber. W. (1965). Pressure Water in the Chad Foermation of Bornu and Dikwa Emirates, North-Eastern Nigeria. Geology Survey of Nigeria Bulletin, NO.35, 138p.

Barber. W and Jone, D.G. (1960). The Geology and Hydrology of Maiduguri, Bornu Province. Geology Survey of Nigeria 1958, pp 5-20.

Bayewu, O. O. (2011). Application of Electrical Resistivity Imaging in delineating a non comformity around Ijesha Ijebu Sourthwestern Nigeria. Jornal of Petroleum and Gas Exploration Reasearch, Vol 2 PP 010-016.

Falconer. J. N. (1911). The Geology and Geography of Northern Nigeria. Universal Journal of Geoscience, Volume 2, pp 13- 54.

Frohlich, R.K., Fisher, J.J. and Summerly, E.(1996). Electric- hydraulic conductivity correlation in fractured crystalline bedrock: central landfill, Rhode Island, USA. Journal of Applied Geophysics, 35: 249-259.

Grant, N.K.,1969. The late Precambrian to early Paleozoic Pan-African Orogeny in Ghana,Togo, Dahomey and Nigeria. Geology Society. Am. Bull., Volume 80, pp45-56.

Hazell, J.R.T., Cratchley C.R. and Jones, C.R.C. (1992). The hydrogeology of crystalline aquifer in Northern Nigeria and Geophysical techniques used in their exploration. In wright G. P. and Burgess W.G. (Eds) the hydrogeology of crystalline Basement Aquifers in Africa. Geological society special publication No. 66.

Jones, R. C. Sarah, B. (1998). The Combined EMT/VES Geophysical Method for sitting Boreholes 54-63.

Kelly, W.E. (1993). Applied Geophysics in hydrogeological and engineering practice. Elsevier, Amsterdam. pp 292-293.

KNARDA,Kano State Agricultural and Rural Development Authority. (1989). Rural water supply project, Vol. II, Summary of Hydrogeological Data. Final Report, WARDROP Engineering Inc. 24 pp. plus Appendices.

Kogbe, C.A (1989). Geology of Nigeria. Rock View (Nigeria) Limited, plot 1234, Zaramaganda, Jos, Nigeria.pp 348 – 358.

Lowrie, W. (1997). Fundamentals of Geophysics. Cambridge University press, United Kingdom. pp 10 - 57.

Mackay. R.A., Greenwood, R. and Rockinggham, J.E. (1952). The Geology of the Plateau tinsfields Re-survey 1945- 1948 Bulletin Geological Survey.

McCurry,P. (1970). Geology of degree sheet 21 Zaria, Nigeria. Unpublished M.Sc thesis, Department of Geology, Ahmadu Bello University, Zaria, Nigeria.

Ogunmola, J.K., Adeofun, C.O., Ogbole, J.O., Goki, N.G., and Ohia, J.A.,(2008). The use of Nigeria SAT-1 and GIS in assessing the mineral potential of raffin-gabbas, north central Nigeria. Middle-east Journal of Scientific Research,3(3), 164-170, IDOSI Publication.

Olugbenga, A.F. (2009). Two dimensional shallow resistivity investigation of the groundwater potential at Nuhu Bamalli Polytechnics. Pacific Journal of Science and Technology, 10(1): 602-613.

Shemang, E.M. (1990). Electrical depth sounding at selected well sites within kubanni River basin Zaria, (unpublished) M.Sc. thesis, Department of Physics, Ahmadu Bello University, Zaria.

Tahir, S. (2011). Resistvity sounding and Borehole Drilling at Sauna Quarters Kano (unpublished) Borehole report

Telford, W.M., Geldart L.P. and Sheriff R.E. (1990). Applied geophysics. Cambridge University Press, London. pp 522 - 577.

Thomas, W.B. (1986). Groundwater occurrence, development and protection. The institution of water engineers and scientists, 31- 33 High Holborn, London WC IV 6AX, England.

Wright, J.B, and McCurry, P.(1970). A reappraisal of some aspects of Precambrian shield geology - discussion. Bull. Geol. Soc. Am., 81: 3491-3492.

APPENDIX 1

Interpreted model and lithology

PROFILE A

STATION	SEQUENCE	RESISTIVITY (Ωm)	THICKNESS (m)	DEPTH (m)	LITHOLOGY
	1	4693	0.993	0.993	LATERITE
A1	2	767			FRACTURED BASEMENT
A2	1	3386	0.225	0.225	LATERITE

	2	10	0.788	1.013	CLAY
	3	1458			FRESH BASEMENT
	1	58	0.697	0.697	SAND
A3	2	738			FRACTURED BASEMENT
	1	35	2.168	2.168	SAND
	2	4	4.775	6.943	CLAY
A4	3	293			FRACTURED BASEMENT
	1	75	4.680	4.680	SAND
	2	4	1.351	6.031	CLAY
A5	3	11223			FRESH BASEMENT
	1	67	4.681	4.681	SAND
	2	4	1.786	6.467	CLAY
A6	3	11142			FRESH BASEMENT
	1	76	2.635	2.635	SAND
	2	181	15.979	18.614	FRACTURED BASEMENT
A7	3	1617			FRESH BASEMENT
	1	92	13.760	13.760	SAND
A8	2	876			FRACTURED BASEMENT
	1	5	2.900	2.900	CLAY
	2	44	26.660	29.560	SAND
A9	3	7677			FRESH BASEMENT
	1	43	26.930	26.930	SAND
A10	2	18861			FRESH BASEMENT
	1	28	2.100	2.100	SAND
	2	10	4.600	6.700	CLAY
A11	3	20672			FRESH BASEMENT
	1	81	2.036	2.210	SAND
	2	9	6.687	8.633	CLAY
A12	3	14188			FRESH BASEMENT

PROFILE B

STATION	SEQUENCE	RESISTIVITY (Ωm)	THICKNESS (m)	DEPTH (m)	LITHOLOGY
	1	485	25.483	25.483	FRACTURED BASEMENT
B1	2	921			FRESH BASEMENT
	1	366	3.480	3.480	FRACTURED BASEMENT
B2	2	2445			FRESH BASEMENT

	1	4008	1.007	1.007	LATERITE
	2	25	4.501	5.508	SAND
B3	3	68161			FRESH BASEMENT
	1	2700	0.997	0.997	LATERITE
	2	20	7.455	8.452	SAND
B4	2	45899			FRESH BASEMENT
	1	37	17.446	17.446	SAND
B5	2	6441			FRESH BASEMENT
	1	33	18.423	18.423	SAND
B6	2	11842			FRESH BASEMENT
	1	1283	1.020	1.020	LATERITE
	2	24	4.736	5.756	SAND
B7	3	21492			FRESH BASEMENT
	1	1074	1.201	1.201	LATERITE
	2	21	5.190	6.391	SAND
B8	3	14632			FRESH BASEMENT
	1	85	10.320	10.320	SAND
B9	2	52595			FRESH BASEMENT
	1	79	5.010	5.010	SAND
B10	2	26911			FRESH BASEMENT
	1	2142	1.510	1.510	LATERITE
B11	2	505			FRACTURED BASEMENT
	1	325	2.894	2.894	FRACTURED BASEMENT
B12	2	1060			FRES BASEMENT

APPENDIX 2

VES A1

S/N	L(m)	b(m)	K (m)	R(Ω)	APP. RES. (ohm-meter)
1	1.5	0.5	6.2832	490.000	3078.7680
2	2.0	0.5	11.7810	184.000	2167.7040
3	3.0	0.5	27.4889	60.900	1674.0764
4	4.5	0.5	62.8319	14.400	904.7794
5	7.0	0.5	153.1526	4.630	709.0965
6	10.0	0.5	313.3739	2.170	680.0214
7	15.0	2.0	173.5730	3.570	619.6556
8	20.0	2.0	311.0177	2.110	656.2473
9	30.0	2.0	703.7168	1.150	809.2743
10	45.0	2.0	1587.2897	0.578	917.4534
11	60.0	2.0	2824.2918	0.413	1166.4325
12	70.0	2.0	3845.3094	0.208	799.8244

VES A2

S/N	L(m)	b(m)	K (m)	R(Ω)	APP. RES. (ohm-meter)
1	1.5	0.5	6.2832	178.000	1118.4096
2	2.0	0.5	11.7810	231.000	2721.4110
3	3.0	0.5	27.4889	0.502	13.7994
4	4.5	0.5	62.8319	0.170	10.6814
5	7.0	0.5	153.1526	0.968	148.2517
6	10.0	0.5	313.3739	2.250	705.0913
7	15.0	2.0	173.5730	2.740	475.5900
8	20.0	2.0	311.0177	1.840	572.2726
9	30.0	2.0	703.7168	0.470	330.7469
10	45.0	2.0	1587.2897	0.280	444.4411
11	60.0	2.0	2824.2918	0.255	720.1944
12	70.0	2.0	3845.3094	0.094	360.6900

VES A3

S/N	L(m)	b(m)	K (m)	R(Ω)	APP. RES. (ohm-meter)
1	1.5	0.5	6.2832	10.900	68.4869
2	2.0	0.5	11.7810	13.400	157.8654
3	3.0	0.5	27.4889	7.820	214.9635
4	4.5	0.5	62.8319	1.460	91.7346
5	7.0	0.5	153.1526	9.000	1378.3734
6	10.0	0.5	313.3739	11.500	3603.7999
7	15.0	2.0	173.5730	3.160	548.4907
8	20.0	2.0	311.0177	9.690	3013.7615
9	30.0	2.0	703.7168	2.350	1653.7345
10	45.0	2.0	1587.2897	0.425	674.5981
11	60.0	2.0	2824.2918	0.248	700.4244
12	70.0	2.0	3845.3094	10.720	41221.7168

VES A4

S/N	L(m)	b(m)	K (m)	R(Ω)	APP. RES. (ohm-meter)
1	1.5	0.5	6.2832	12.800	80.4250
2	2.0	0.5	11.7810	17.500	206.1675
3	3.0	0.5	27.4889	9.280	255.0974
4	4.5	0.5	62.8319	3.730	234.3630
5	7.0	0.5	153.1526	1.570	240.4496
6	10.0	0.5	313.3739	0.805	252.2660
7	15.0	2.0	173.5730	0.983	170.6223
8	20.0	2.0	311.0177	0.569	176.9691
9	30.0	2.0	703.7168	0.017	12.2447
10	45.0	2.0	1587.2897	0.018	29.0474
11	60.0	2.0	2824.2918	0.537	1516.6447
12	70.0	2.0	3845.3094	2.650	10190.0699

VES A5

S/N	L(m)	b(m)	K (m)	R(Ω)	APP. RES. (ohm-meter)
1	1.5	0.5	6.2832	17.800	111.8410
2	2.0	0.5	11.7810	3.350	39.4664
3	3.0	0.5	27.4889	2.730	75.0448
4	4.5	0.5	62.8319	1.670	104.9293
5	7.0	0.5	153.1526	0.470	71.9817
6	10.0	0.5	313.3739	0.188	58.9143
7	15.0	2.0	173.5730	0.377	65.4370
8	20.0	2.0	311.0177	0.199	61.8925
9	30.0	2.0	703.7168	0.083	58.2678
10	45.0	2.0	1587.2897	0.069	109.5230
11	60.0	2.0	2824.2918	0.023	65.2411
12	70.0	2.0	3845.3094	0.995	3826.0829

VES A6

S/N	L(m)	b(m)	K (m)	R(Ω)	APP. RES. (ohm-meter)
1	1.5	0.5	6.2832	14.240	89.4703
2	2.0	0.5	11.7810	2.130	25.0924
3	3.0	0.5	27.4889	2.570	70.6411
4	4.5	0.5	62.8319	1.559	97.9612
5	7.0	0.5	153.1526	0.450	68.9187
6	10.0	0.5	313.3739	0.166	52.0201
7	15.0	2.0	173.5730	0.347	60.2125
8	20.0	2.0	311.0177	0.187	58.1603
9	30.0	2.0	703.7168	0.083	58.1974

10	45.0	2.0	1587.2897	0.062	98.4120
11	60.0	2.0	2824.2918	0.023	63.5466
12	70.0	2.0	3845.3094	0.999	3841.4640

VES A7

S/N	L(m)	b(m)	K (m)	R(Ω)	APP. RES (ohm-meter)
1	1.5	0.5	6.2832	16.200	101.7878
2	2.0	0.5	11.7810	5.320	62.6749
3	3.0	0.5	27.4889	2.700	74.2201
4	4.5	0.5	62.8319	1.570	98.6461
5	7.0	0.5	153.1526	0.772	118.2338
6	10.0	0.5	313.3739	0.421	131.9304
7	15.0	2.0	173.5730	1.090	189.1946
8	20.0	2.0	311.0177	0.466	144.9342
9	30.0	2.0	703.7168	0.145	102.0389
10	45.0	2.0	1587.2897	0.223	353.9656
11	60.0	2.0	2824.2918	0.129	364.3336
12	70.0	2.0	3845.3094	0.019	73.0609

VES A8

S/N	L(m)	b(m)	K (m)	R(Ω)	APP. RES. (ohm-meter)
1	1.5	0.5	6.2832	15.900	99.8997
2	2.0	0.5	11.7810	5.229	61.6064

3	3.0	0.5	27.4889	2.500	68.7196
4	4.5	0.5	62.8319	1.5499	97.3832
5	7.0	0.5	153.1526	0.770	117.8969
6	10.0	0.5	313.3739	0.415	129.9875
7	15.0	2.0	173.5730	1.020	176.9924
8	20.0	2.0	311.0177	0.442	137.4076
9	30.0	2.0	703.7168	0.140	98.52035
10	45.0	2.0	1587.2897	0.222	352.3783
11	60.0	2.0	2824.2918	0.126	354.7311
12	70.0	2.0	3845.3094	0.014	53.8343

VES A9

S/N	L(m)	b(m)	K (m)	R(Ω)	APP. RES. (ohm-meter)
1	1.5	0.5	6.2832	5.440	34.1806
2	2.0	0.5	11.7810	4.630	54.5460
3	3.0	0.5	27.4889	1.640	45.0819
4	4.5	0.5	62.8319	0.726	45.6160
5	7.0	0.5	153.1526	0.318	48.7025
6	10.0	0.5	313.3739	0.374	117.2018
7	15.0	2.0	173.5730	0.130	22.5645
8	20.0	2.0	311.0177	0.113	35.1450
9	30.0	2.0	703.7168	0.038	27.0227
10	45.0	2.0	1587.2897	0.064	101.5865
11	60.0	2.0	2824.2918	0.014	38.6928
12	70.0	2.0	3845.3094	0.058	221.1053

VES 10

S/N	L(m)	b(m)	K (m)	R(Ω)	APP. RES. (ohm-meter)
1	1.5	0.5	6.2832	5.159	32.4150
2	2.0	0.5	11.7810	4.850	57.1379
3	3.0	0.5	27.4889	1.670	45.9065

4	4.5	0.5	62.8319	0.729	45.8045
5	7.0	0.5	153.1526	0.312	47.7836
6	10.0	0.5	313.3739	0.378	118.4553
7	15.0	2.0	173.5730	0.119	20.6552
8	20.0	2.0	311.0177	0.111	34.5230
9	30.0	2.0	703.7168	0.037	26.0375
10	45.0	2.0	1587.2897	0.063	99.8405
11	60.0	2.0	2824.2918	0.013	36.1509
12	70.0	2.0	3845.3094	0.057	217.2600

VES A11

S/N	L(m)	b(m)	K (m)	R(Ω)	APP. RES. (ohm-meter)
1	1.5	0.5	6.2832	429.000	2695.4928
2	2.0	0.5	11.7810	181.000	2132.3610
3	3.0	0.5	27.4889	86.100	2366.7977
4	4.5	0.5	62.8319	18.700	1174.9565
5	7.0	0.5	153.1526	1.600	245.0442
6	10.0	0.5	313.3739	0.332	104.0401
7	15.0	2.0	173.5730	0.372	64.5692
8	20.0	2.0	311.0177	0.053	16.3595
9	30.0	2.0	703.7168	0.028	19.3522
10	45.0	2.0	1587.2897	0.083	132.2212
11	60.0	2.0	2824.2918	0.271	765.3831
12	70.0	2.0	3845.3094	0.038	145.3527

VES 12

S/N	L(m)	b(m)	K (m)	R(Ω)	APP. RES. (ohm-meter)
1	1.5	0.5	6.2832	178.000	1118.4096
2	2.0	0.5	11.7810	63.500	748.0935
3	3.0	0.5	27.4889	22.500	618.5012
4	4.5	0.5	62.8319	4.010	251.9559
5	7.0	0.5	153.1526	0.884	135.3869
6	10.0	0.5	313.3739	0.194	60.7945
7	15.0	2.0	173.5730	0.104	18.0516
8	20.0	2.0	311.0177	0.129	40.1213
9	30.0	2.0	703.7168	0.023	16.1151
10	45.0	2.0	1587.2897	0.011	18.0951
11	60.0	2.0	2824.2918	0.027	75.1262
12	70.0	2.0	3845.3094	0.283	1088.2226

VES B1

S/N	L(m)	b(m)	K (m)	R(Ω)	APP. RES. (ohm-meter)
1	1.5	0.5	6.2832	143.000	898.4976
2	2.0	0.5	11.7810	41.000	483.0210
3	3.0	0.5	27.4889	14.600	401.3385
4	4.5	0.5	62.8319	5.000	314.1595
5	7.0	0.5	153.1526	1.930	295.5845
6	10.0	0.5	313.3739	2.140	670.6201
7	15.0	2.0	173.5730	1.430	248.2094
8	20.0	2.0	311.0177	1.260	391.8823
9	30.0	2.0	703.7168	0.876	616.4559
10	45.0	2.0	1587.2897	0.546	866.6602
11	60.0	2.0	2824.2918	0.206	581.8041
12	70.0	2.0	3845.3094	0.084	323.0060

VES B2

S/N	L(m)	b(m)	K (m)	R(Ω)	APP. RES. (ohm-meter)
1	1.5	0.5	6.2832	66.000	414.6912
2	2.0	0.5	11.7810	26.800	315.7308
3	3.0	0.5	27.4889	14.700	404.0874
4	4.5	0.5	62.8319	6.670	419.0888
5	7.0	0.5	153.1526	3.480	532.9710
6	10.0	0.5	313.3739	2.190	686.2888
7	15.0	2.0	173.5730	4.940	857.4506
8	20.0	2.0	311.0177	3.370	1048.1296
9	30.0	2.0	703.7168	1.930	1358.1734
10	45.0	2.0	1587.2897	1.040	1650.7813
11	60.0	2.0	2824.2918	0.650	1835.7897
12	70.0	2.0	3845.3094	0.576	2214.8982

VES B3

S/N	L(m)	b(m)	K (m)	R(Ω)	APP. RES. (ohm-meter)
1	1.5	0.5	6.2832	263.000	1652.4816
2	2.0	0.5	11.7810	866.000	10202.3460
3	3.0	0.5	27.4889	186.000	5112.9428
4	4.5	0.5	62.8319	1.790	112.4691
5	7.0	0.5	153.1526	0.770	117.9275
6	10.0	0.5	313.3739	0.234	73.3295
7	15.0	2.0	173.5730	0.256	44.4347
8	20.0	2.0	311.0177	0.333	103.5689
9	30.0	2.0	703.7168	0.138	97.1129
10	45.0	2.0	1587.2897	0.068	107.4595
11	60.0	2.0	2824.2918	0.057	161.2671
12	70.0	2.0	3845.3094	0.491	1888.0469

VES B4

S/N	L(m)	b(m)	K (m)	R(Ω)	APP. RES. (ohm-meter)
1	1.5	0.5	6.2832	802.000	5039.1264
2	2.0	0.5	11.7810	444.000	5230.7640
3	3.0	0.5	27.4889	138.000	3793.4737
4	4.5	0.5	62.8319	25.500	1602.2135
5	7.0	0.5	153.1526	3.890	595.7636
6	10.0	0.5	313.3739	0.289	90.5651
7	15.0	2.0	173.5730	0.546	94.7709
8	20.0	2.0	311.0177	0.024	7.4022
9	30.0	2.0	703.7168	0.042	29.6265
10	45.0	2.0	1587.2897	0.027	42.8568
11	60.0	2.0	2824.2918	0.031	86.1409
12	70.0	2.0	3845.3094	0.047	180.7295

VES B5

S/N	L(m)	b(m)	K (m)	R(Ω)	APP. RES. (ohm-meter)
1	1.5	0.5	6.2832	6.020	37.8249
2	2.0	0.5	11.7810	5.830	68.6832
3	3.0	0.5	27.4889	1.260	34.6361
4	4.5	0.5	62.8319	0.608	38.2018
5	7.0	0.5	153.1526	0.210	32.1621
6	10.0	0.5	313.3739	0.637	199.6192
7	15.0	2.0	173.5730	0.128	22.2173
8	20.0	2.0	311.0177	0.109	33.9009
9	30.0	2.0	703.7168	0.033	23.4338

10	45.0	2.0	1587.2897	0.062	98.4120
11	60.0	2.0	2824.2918	0.014	39.5401
12	70.0	2.0	3845.3094	0.042	161.5030

VES B6

S/N	L(m)	b(m)	K (m)	R(Ω)	APP. RES. (ohm-meter)
1	1.5	0.5	6.2832	5.980	37.5735
2	2.0	0.5	11.7810	5.740	67.6229
3	3.0	0.5	27.4889	1.200	32.9867
4	4.5	0.5	62.8319	0.599	37.6363
5	7.0	0.5	153.1526	0.189	28.9458
6	10.0	0.5	313.3739	0.637	199.619
7	15.0	2.0	173.5730	0.125	21.6966
8	20.0	2.0	311.0177	0.105	32.6569
9	30.0	2.0	703.7168	0.032	22.7301
10	45.0	2.0	1587.2897	0.060	95.0787
11	60.0	2.0	2824.2918	0.012	33.6091
12	70.0	2.0	3845.3094	0.040	153.4278

VES B7

S/N	L(m)	b(m)	K (m)	R(Ω)	APP. RES. (ohm-meter)
1	1.5	0.5	6.2832	194.000	1218.9410
2	2.0	0.5	11.7810	50.000	589.0500
3	3.0	0.5	27.4889	6.760	185.8252
4	4.5	0.5	62.8319	2.010	126.2921
5	7.0	0.5	153.1526	0.290	44.4143

6	10.0	0.5	313.3739	0.086	26.9502
7	15.0	2.0	173.5730	0.313	54.3284
8	20.0	2.0	311.0177	0.358	111.3443
9	30.0	2.0	703.7168	0.413	290.6350
10	45.0	2.0	1587.2897	0.041	65.5551
11	60.0	2.0	2824.2918	0.118	333.2664
12	70.0	2.0	3845.3094	0.089	343.0016

VES B8

S/N	L(m)	b(m)	K (m)	R(Ω)	APP. RES. (ohm-meter)
1	1.5	0.5	6.2832	180.000	1130.9760
2	2.0	0.5	11.7810	48.900	576.0909
3	3.0	0.5	27.4889	5.970	164.1090
4	4.5	0.5	62.8319	2.020	126.9204
5	7.0	0.5	153.1526	0.259	39.6665
6	10.0	0.5	313.3739	0.082	25.6653
7	15.0	2.0	173.5730	0.299	51.8983
8	20.0	2.0	311.0177	0.082	25.4724
9	30.0	2.0	703.7168	0.417	293.4499
10	45.0	2.0	1587.2897	0.041	64.7614
11	60.0	2.0	2824.2918	0.115	324.7936
12	70.0	2.0	3845.3094	0.089	341.8480

VES B9

S/N	L(m)	b(m)	K (m)	R(Ω)	APP. RES. (ohm-meter)
1	1.5	0.5	6.2832	43.800	275.2042

2	2.0	0.5	11.7810	10.400	122.5224
3	3.0	0.5	27.4889	2.710	74.4951
4	4.5	0.5	62.8319	0.921	57.8682
5	7.0	0.5	153.1526	0.371	56.8196
6	10.0	0.5	313.3739	0.186	58.2876
7	15.0	2.0	173.5730	0.641	111.2603
8	20.0	2.0	311.0177	0.227	70.6010
9	30.0	2.0	703.7168	0.103	72.4828
10	45.0	2.0	1587.2897	0.024	37.3013
11	60.0	2.0	2824.2918	4.050	11438.3800
12	70.0	2.0	3845.3094	7.530	28955.1800

VES B10

S/N	L(m)	b(m)	K (m)	R(Ω)	APP. RES. (ohm-meter)
1	1.5	0.5	6.2832	42.200	265.1510
2	2.0	0.5	11.7810	10.090	110.9456
3	3.0	0.5	27.4889	2.699	74.1926
4	4.5	0.5	62.8319	0.919	57.7425
5	7.0	0.5	153.1526	0.368	56.3602
6	10.0	0.5	313.3739	0.018	5.7661
7	15.0	2.0	173.5730	0.638	110.7396
8	20.0	2.0	311.0177	0.222	69.0459
9	30.0	2.0	703.7168	0.101	71.0754
10	45.0	2.0	1587.2897	0.023	36.6664
11	60.0	2.0	2824.2918	3.890	10986.4951
12	70.0	2.0	3845.3094	7.319	28143.8195

VES B11

S/N	L(m)	b(m)	K (m)	R(Ω)	APP. RES. (ohm-meter)
1	1.5	0.5	6.2832	384.000	2412.7490
2	2.0	0.5	11.7810	88.400	1041.4400
3	3.0	0.5	27.4889	34.400	945.6195
4	4.5	0.5	62.8319	12.400	779.1156
5	7.0	0.5	153.1526	4.840	741.2586
6	10.0	0.5	313.3739	1.530	479.4621
7	15.0	2.0	173.5730	1.980	343.6745
8	20.0	2.0	311.0177	1.550	482.0774
9	30.0	2.0	703.7168	0.860	605.1964
10	45.0	2.0	1587.2897	0.355	563.4878
11	60.0	2.0	2824.2918	0.174	491.4268
12	70.0	2.0	3845.3094	0.072	276.8623

VES B12

S/N	L(m)	b(m)	K (m)	R(Ω)	APP. RES. (ohm-meter)
1	1.5	0.5	6.2832	69.600	437.3107
2	2.0	0.5	11.7810	24.800	292.1688
3	3.0	0.5	27.4889	10.900	299.6294
4	4.5	0.5	62.8319	6.200	389.5578
5	7.0	0.5	153.1526	3.780	578.9168
6	10.0	0.5	313.3739	2.220	695.6901
7	15.0	2.0	173.5730	3.790	657.8417
8	20.0	2.0	311.0177	2.490	774.4341
9	30.0	2.0	703.7168	1.380	971.1292
10	45.0	2.0	1587.2897	0.586	930.1518
11	60.0	2.0	2824.2918	0.362	1022.3940
12	70.0	2.0	3845.3094	0.040	154.5814

APPENDIX 3

SOUNDING CURVES AND INTERPRETED MODELS